Title: Marine heatwaves disrupt ecosystem structure and function via altered food webs and energy flux

Authors: Dylan G.E. Gomes[1,2*], James J. Ruzicka[3], Lisa G. Crozier[4], David D. Huff[5], Richard D. Brodeur[5], Joshua D. Stewart[1]

Affiliations:

[1] Ocean Ecology Lab, Marine Mammal Institute, Oregon State University; Newport, OR, 97365, USA

[2] National Academy of Sciences NRC Postdoctoral Research Associateship, Northwest Fisheries Science Center, National Marine Fisheries Service, National Oceanic and Atmospheric Administration; Seattle, WA, 98112, USA

[3] Ecosystem Sciences Division, Pacific Islands Fisheries Science Center, National Marine Fisheries Service, National Oceanic and Atmospheric Administration; Honolulu, HI, 96822, USA

[4] Fish Ecology Division, Northwest Fisheries Science Center, National Marine Fisheries Service, National Oceanic and Atmospheric Administration; Seattle, WA, 98112, USA

[5] Fish Ecology Division, Northwest Fisheries Science Center, National Marine Fisheries Service, National Oceanic and Atmospheric Administration; Newport, OR, 97365, USA

[*] Corresponding author. Email: dylan.ge.gomes@gmail.com

Abstract: The prevalence and intensity of marine heatwaves is increasing globally, disrupting local environmental conditions. The individual and population-level impacts of prolonged heatwaves on marine species have recently been demonstrated, yet whole-ecosystem consequences remain unexplored. We compare ecosystem models parameterized before and after the onset of recent heatwaves to evaluate the cascading effects on ecosystem structure and function in the Northeast Pacific Ocean. While the ecosystem-level contribution, as prey, and demand, as predators, of most functional groups changed, gelatinous taxa experienced the largest transformations, underscored by the arrival of northward-expanding pyrosomes. Despite altered trophic relationships and energy flux, the post-heatwave ecosystem appears stable, suggesting a shift to a novel ecosystem state, with potentially profound consequences for ecosystem structure, energy flows, and threatened and harvested species.

Main Text:

Marine heatwaves (MHWs) are periods of prolonged, unusually warm ocean temperatures that can have significant impacts on marine ecosystems[1–4]. In tropical systems, sustained periods of warm water can cause coral bleaching and mass mortality events, which likely affects entire communities that rely on the complex structure and ecosystem functions provided by live coral[5]. In temperate systems, ocean temperature increases can lead to harmful algal blooms that produce toxins that kill other marine organisms[6,7]. These algae blooms can also lead to widespread hypoxic events, contributing to recent increases in the occurrence of ecological 'dead zones' that affect a wide range of species[8]. MHWs can alter nutrient cycling and availability in the ocean, which can affect the growth of phytoplankton. These bottom-up processes can alter lower trophic level productivity, which may in turn lead to stress and starvation in top predators, ultimately affecting reproductive success[9,10]. Cumulative impacts can lead to poleward distribution shifts of many pelagic species[11–13], resulting in disrupted or novel communities and changes in predator-prey relationships, which likely leads to changes in the overall structure of marine ecosystems as a consequence of MHWs. However, the full ecosystem-scale effects of MHWs have not been estimated within an impacted system to date, leaving substantial uncertainty in the short- and long-term consequences of MHWs on ecosystem structure and function.

The Northern California Current marine ecosystem extends from Vancouver Island, British Columbia, Canada to Cape Mendocino, California, United States. It is a highly productive upwelling marine ecosystem that supports high biomass of marine species, many of which are harvested in economically and socially important fisheries[14]. Sea surface temperatures in the ecosystem have been anomalously high in recent years, starting with the warm water "blob" in

the winter of 2013-2014[15–17], which was among the most intense MHWs ever recorded[1]. Re-occurring MHWs have kept much of the North Pacific Ocean in a state of anomalously warm conditions over the past decade, indicating that these novel conditions are perhaps the new normal[18–20].

These anomalously warm periods have led to documented changes in the abundance and distribution of diverse taxa including gelatinous invertebrates, copepods, krill, squid, fishes and sharks[19,21–27], and have impacted important fisheries[28]. Extreme warming events within the Northern California Current are expected to be exacerbated by climate change in complex and potentially non-linear ways[29,30]. Yet the ecosystem-wide ramifications of such sudden events are likely to be far greater than the expected changes due to long-term warming alone[31].

Here, we compare two end-to-end ecosystem food web models of the Northern California Current representing time periods immediately preceding (1999-2012) and following (2014-2022) recent marine heatwaves [pre-heatwave and post-heatwave, respectively[32–34]] to make inferences about ecosystem-level changes that have occurred since the onset of these recent extreme warming events. We estimate the effects of MHWs on the energy flow between producers and consumers across scales from individual functional groups to the entire food web network. Accounting for energy flux within the entire ecosystem allows us to directly estimate the cascading, ecosystem-wide effects of temperature-induced changes through both direct and indirect food web pathways.

Leveraging time series abundance data of 361 taxa (grouped into 86 functional groups) from six long term surveys, diet information from a new diet database[35], and previous modeling efforts,

we built two food web networks (pre-MHW and post-MHW) using an extension of the popular Ecopath ecosystem modeling framework (Ecotran[32,33,36]). Our comparative analysis of these two food web networks shows that lower trophic level biomass and energy pathways experienced greater changes after MHWs than upper trophic levels (Figs. 1, 2), but that the energetic consumption (of lower trophic levels) and energetic contribution (to higher trophic levels) of many functional groups significantly changed between pre- and post-MHW time periods (Figs. 3, S1-S5). Predators consumed prey both in different absolute quantities and proportions before compared with after the MHWs (Fig. 2).

By directly estimating changes in both biomass and trophic interactions across the entire ecosystem, we find that the largest perturbation to the energy flux of the Northern California Current ecosystem since the onset of the 2013-2014 marine heatwave is driven by a dramatic increase in the abundance of pyrosomes, *Pyrosoma atlanticum* (Fig. 1, Table S1). This gelatinous species was essentially absent from the Northern California Current prior to recent MHWs[37–39], and this rapid increase drove substantial changes throughout the food web at low and mid trophic levels as pyrosomes consumed energy that would have been available for other groups (Fig. 1). Species at the base of the food web, such as pteropods, pelagic amphipods, small invertebrate larvae, small mesh-feeding jellies, krill, and sardine all consumed less phytoplankton in the post-MHW period, which led to decreases in their abundances. This, in turn, left less forage for the carnivorous and larger jellies, which also declined (Figs. 1, 3).

Further, our models suggest that the majority of this re-directed energy does not flow to higher trophic levels, with more than 98% of pyrosome biomass ending up in detritus pools (Figs. 1, 2).

Although there is evidence that some predators have consumed pyrosomes and other abundant gelatinous taxa during the MHW[22,40], it is not clear what energetic benefits accrue to these predators compared to feeding on crustacean or fish prey. It has long been assumed that gelatinous prey are trophic dead ends, due to their low energy content[41], although advances in more recent methods suggest that gelatinous prey might be more important than previously believed[42]. In the Northern California Current, it appears that pyrosomes are not consumed as readily as jellies. This may be because they are more difficult to digest, offer lower energy content, or remain novel to the food web such that predators have not yet responded. Thus, while overall gelatinous biomass in the ecosystem increased, the boom in scarcely consumed pyrosomes along with the concurrent decrease in jelly abundance has led to a marked decrease in the overall consumption of gelatinous prey since the onset of MHWs (Figs. 1, 2). More generally, a persistent shift toward filter-feeding gelatinous zooplankton and away from omnivorous euphausiids could have major negative implications for higher trophic levels including commercially important fishes, and thus food security in many ecosystems[43]. This further highlights the importance of understanding the uncertainty in the trophic influence of pyrosomes in their recently expanded northward range shift, the outcome of which will have important consequences for the future of the Northern California Current ecosystem under intensifying global warming.

It is possible that the observed transition to pyrosome dominance represents a novel biological regime shift, in which the increase in a new species creates an altered food web structure that is stable. Despite large shifts in biomass and connections of lower trophic levels (Fig. 1), the average trophic level did not change across models (Table 1). Higher average trophic levels across a food web signals a more unstable ecosystem[44] while low average trophic levels indicate

a more efficient system as energy is lost at each level of consumption between the base of the food web and a fished species[45,46]. This suggests that the Northern California Current ecosystem remained relatively stable after disruption by repeated MHWs, rather than entering an unstable state characterized by higher mean trophic levels.

The relationship between ecosystem complexity and stability has long been debated[47–51]. The existence of an inverse Complexity-Stability relationship has been argued from graph theory[49,51], yet these arguments have been criticized for relying on unrepresentative networks[48,52]. Real ecosystems, on the other hand, tend to show increased stability with increasing complexity[47,53]. Various network metrics, such as connectance (the number of realized trophic links relative to the total possible number) and link density (the number of links per node) are commonly-used measures of complexity that are thought to relate to the robustness of food webs to disturbances[46,48,53], and offer an independent evaluation of ecosystem stability here. Both network metrics were slightly higher in the post-MHW model, which further suggests that the post-MHW ecosystem is stable (Table 1).

This novel ecosystem state, characterized by increased pyrosome biomass and decreased energy flux to and from other low trophic-level species, may have important implications for fishery management. Chinook salmon and cod for example, appear to have decreased since the onset of the marine heatwaves in the Northern California Current (Fig. 1)[54]. Chinook salmon commercial harvest has been reduced by nearly a factor of three in the Northern California Current since the onset of the MHWs [PacFIN, http://pacfin.psmfc.org][32,33]. Cod do not sustain a major fishery in the Northern California Current, but they are an important fished species just north in Alaska,

where declines have similarly been documented during these recent North Pacific MHWs[4]. If these species do not return to their former abundance and biomass, commercial fisheries may have to shift their efforts towards more readily available species. The increased dominance of Pacific jack mackerel (*Trachurus symmetricus*) in the Northern California Current ecosystem is demonstrated by huge increases in their abundance in recent years (Fig. 1)[24,55]. The impact of jack mackerel on lower trophic levels has increased since the onset of recent marine heatwaves (Figs. 2, 3). Yet, despite this increase in abundance, commercial fisheries in the U.S. have not shown any change in jack mackerel landings [PacFIN, http://pacfin.psmfc.org/][32], which might suggest jack mackerel is an under-utilized resource that can support substantial fishery landings. Adapting harvest strategies to account for changes in ecosystem structure could represent a significant step towards climate-resilient fisheries. However, further work is needed to determine if changes in the abundance of these species are directly influenced by marine heatwaves. Pacific sardine (*Sardinops sagax*) have complicated population fluctuations in response to multiple factors, and are often thought to have a positive relationship with ocean temperatures[56,57]. Yet sardine collapsed just prior to the onset of the MHWs, and populations have not shown signs of rebuilding despite the warm ocean conditions persisting throughout the California Current Ecosystem[58].

As marine heatwaves intensify and are increasingly common, these climate disturbances will have major impacts on marine ecosystems[2] with both winners and losers as some species take advantage of changing conditions or expand their distribution whereas others struggle to adapt or are physiologically constrained[59]. Estimating changes to energy flow within ecosystems and the energetic consumption and contribution of individual functional groups provides an approach for quantifying ecosystem changes as global warming increasingly disrupts food webs and the

sustainable use of such resources. Ecosystem models may provide a means for determining whether disrupted marine ecosystems have entered an alternative stable state or are temporary instabilities, based on network metrics of stability and trophic connections. Thus, these tools may allow us to better predict future winners and losers as we prepare for climate resiliency in ecosystem-based fisheries management and the recovery of threatened and protected species in ecologically and economically important ecosystems.

Methods

EcoTran

Pre-MHW and post-MHW were built and analyzed within the EcoTran end-to-end ecosystem model platform[36]. EcoTran builds upon the widely-used Ecopath food web modeling framework[60]. One NCC ecosystem model was parameterized from datasets collected prior to the 2014 onset of MHW[33] and the other model was developed recently, which is based on datasets from 2014 onwards through multiple warm ocean years[32]. Both models represent 80 living functional groups, 3 nutrient pools, 5 detritus pools, and 2 fisheries. The trophic interactions within each model are described as a production matrix defining the fate of all consumption by each group between its metabolic costs, non-assimilated egestion, biomass production that is consumed by each predator or fleet, and senescence[32,33,61].

Model adjustment details

The pre-MHW model, adapted from Ruzicka et al. (2012), was updated in several ways. First, Ruzicka et al. (2012) used Ecopath methods to estimate the biomass of euphausiids required to to maintain the pre-MHW food web in thermodynamic balance[33]. Since then, a longer

and more precise euphausiid time series has been developed from the Joint U.S.-Canada Integrated Ecosystem and Pacific Hake Acoustic Trawl Survey and modeling efforts[62]. In the post-MHW model, Gomes et al. (2022) used euphausiid biomass densities from the 2015, 2017, and 2019 surveys. The pre-MHW model was updated to use the earlier period of the time series (2007, 2009, 2011, and 2012). Similarly, Ecopath-based estimates of invertebrate egg biomasses were dramatically different between the pre- and post-MHW models[32,33]. We used survey data from the Newport Hydrographic Line (NHL) to parameterize invertebrate eggs in the pre-MHW (NHL data: 2000-2012) and post-MHW (NHL data: 2014-2020) models. Due to the changes in biomass between the previously published pre-MHW model and the one used here we needed to re-balance the ecopath model because phytoplankton were slightly over-consumed by the increase in euphausiids. We accomplished this with small changes to the diet matrix of the pre-MHW model to move pressure off of phytoplankton (see supplemental "preMHW_DietChanges.csv"). See previous food web models for more information about data used, model-building, and mass-balancing procedures[32,33].

Due to slight differences in the food web model structure between the pre- and post-MHW ecosystem models, it was necessary to combine some functional groups to make comparisons across the models (see Table S1). For all groups that were combined, diets were aggregated as a weighted averaging (weighted by biomass of individual components/species of the functional group). Total functional group biomasses (for mass-balancing) were summed across the constituent components/species within each functional group. Pyrosomes are not thought to have been present in the pre-MHW period in the NCC ecosystem[39], but to make models directly comparable, we added a trace amount of pyrosomes to this pre-MHW model (0.00001 mt/km2). Marine mammals from Gomes et al. (2022) were combined to match that of Ruzicka et al. (2012); that is, Northern elephant seals and sea lion (California and Steller's) functional groups

were combined into a large pinniped group and other killer whales and southern resident killer whales were grouped into a killer whale functional group (as they both originally were in Ruzicka et al., 2012). Juvenile salmon groups also did not match between the two ecosystem models; for simplicity, they were combined into four groups within each model: yearling coho, yearling chinook, subyearling chinook, and other juvenile salmonids. Similarly, all commercial fleets were aggregated into one commercial fishery fleet due to recent changes in the PacFIN database fleet names (http://pacfin.psmfc.org/). To see expanded fleet information, please see Ruzicka et al. (2012) and Gomes et al. (2022).

Network analyses and metrics

To compare food web structures pre- and post-MHW, we measured average (arithmetic mean) trophic level, average trophic level weighted by the biomass of each functional group, network connectance (the number of non-zero realized links relative to, i.e., divided by, the total number of possible links; 7396 in an 86 x 86 network), and link density (the average number of connecting links per functional group) (Table 1). The initial food web for the post-MHW model was built upon the pre-MHW model, such that pre-MHW trophic connections were included in the post-MHW along with new diet data[32]. To ensure that the network connectance and link densities were not artificially inflated in the post-MHW period, we removed all trophic connections within the post-MHW network that were originally carried over from the pre-MHW model (and which were not represented in the updated diet data; see supplemental code).

A "difference" network was calculated as the difference between the edges and node biomasses in the pre-MHW model and the post-MHW model (Fig. 1). Node and edge sizes and colors are dependent on the magnitude and direction of change, respectively. Blue signifies a decrease in (from pre-MHW to post-MHW) biomass density (nodes) or energy flow (edges) and

red signifies an increase. Bigger circles indicate (on a log scale) higher differences in biomass and thicker and darker edges denote larger changes in energy flows. The network was visualized with help from the R package `qgraph`[63].

Energetic consumption and contributions

To make comparisons of ecosystem structure between pre- and post-MHW years, steady-state models were used to estimate the relative importance of functional groups for transferring energy to higher trophic levels. We calculated the relevance of targeted functional groups as both consumer (consumption of lower trophic levels) and producer (contribution to next trophic level) with two non-dimensional metrics: footprint and reach, respectively.

A functional group's trophic impact upon lower trophic levels is expressed by its footprint, which is the fraction of each producer group's total production supporting consumer groups via all direct and indirect pathways (excluding detritus). The importance of a functional group to higher trophic levels was expressed by its reach: the fraction of consumers' production that originated with (or passed through) the functional group via all direct and indirect pathways[33].

Footprint and reach can be defined broadly (i.e., the footprint upon all lower trophic levels) or precisely (i.e., the footprint upon one specific producer). For our general ecosystem-wide comparison of the roles of phytoplankton, copepods, euphausiids, forage fishes, gelatinous zooplankton, rockfishes, and fish, seabird, and mammalian predators, we adopted the broadest definitions, considering footprint and reach relative to total system production and total consumer production, respectively.

The net uncertainty among physiological parameters, diet, and nutrient cycling terms are expressed as levels of uncertainty about each element of the production matrix. In our analyses, each element of the production matrix was randomly varied by drawing model parameters from a

normal distribution with a mean of the originally parameterized value and a standard deviation based on standard coefficient of variation (CV) values. We drew 1000 possible Monte Carlo food web models to investigate the propagation of uncertainty for footprint and reach of each assessed functional group within each model (pre- and post-MHW). Footprint and reach values were plotted with help from the R package `ggplot2`[64].

Statistical analysis

Two-tailed t-tests in R[65] were used to compare mean trophic levels, network connectance, link density, and the footprint and reach metrics (for each functional group) across pre- and post-MHW models. Since we made multiple comparisons for footprint and reach metrics (each functional group × both footprint and reach metrics), we corrected p values with conservative Bonferroni corrections. For network connectance and link density, we created 100 bootstrapped networks by randomly sampling, with replacement, which nodes to use, each iteration re-calculating connectance and density, which were then compared across models.

Data Availability and Code Availability:

Open data and code are important[66]. All data, code, and materials used in the analysis[67] are available in a long-term data repository at: https://doi.org/10.5281/zenodo.8121889. Additional ECOTRAN code[68] is available at https://doi.org/10.5281/zenodo.8140850. Additional post-MHW ecosystem model details[69] are available at https://doi.org/10.5281/zenodo.7079777.

Acknowledgments:

We thank Mary Hunsicker and Andrew Thompson for feedback on earlier versions of this manuscript. We thank Elizabeth M. Phillips, Alicia Billings, Cheryl A. Morgan, Jen E. Zamon, Elizabeth A. Daly, Joseph. J. Bizzarro, Jennifer L. Fisher, and Toby Auth for access to NOAA biological survey data.

Funding:

National Academy of Science's National Research Council Postdoctoral Research Associateship Program (DGEG)

Author contributions:

Conceptualization: DGEG, JJR, LGC, DDH, RDB, JDS

Data curation: DGEG, JJR

Formal analysis: DGEG

Funding acquisition: LGC, DDH, DGEG

Investigation: DGEG

Methodology: DGEG, JJR

Project administration: DGEG, JJR, LGC, DDH

Software: DGEG, JJR

Supervision: DGEG, JJR, LGC, DDH, JDS

Validation: DGEG

Visualization: DGEG

Writing – original draft: DGEG

Writing – review & editing: DGEG, JJR, LGC, DDH, RDB, JDS

Competing interests: Authors declare that they have no competing interests.

Correspondence and requests for materials should be addressed to DGEG (dylan.ge.gomes@gmail.com).

References and Notes

1. Hobday, A. J. *et al.* Categorizing and naming marine heatwaves. *Oceanography* **31**, 162–173 (2018).
2. Smale, D. A. *et al.* Marine heatwaves threaten global biodiversity and the provision of ecosystem services. *Nature Climate Change* **9**, 306–312 (2019).
3. Smith, K. E. *et al.* Biological impacts of marine heatwaves. *Annual review of marine science* **15**, 119–145 (2023).
4. Suryan, R. M. *et al.* Ecosystem response persists after a prolonged marine heatwave. *Scientific reports* **11**, 1–17 (2021).
5. Hughes, T. P. *et al.* Spatial and temporal patterns of mass bleaching of corals in the Anthropocene. *Science* **359**, 80–83 (2018).
6. McCabe, R. M. *et al.* An unprecedented coastwide toxic algal bloom linked to anomalous ocean conditions. *Geophysical Research Letters* **43**, 10–366 (2016).
7. Trainer, V. L. *et al.* Pelagic harmful algal blooms and climate change: Lessons from nature's experiments with extremes. *Harmful algae* **91**, 101591 (2020).
8. Diaz, R. J. & Rosenberg, R. Spreading dead zones and consequences for marine ecosystems. *science* **321**, 926–929 (2008).
9. Oliver, E. C. *et al.* Longer and more frequent marine heatwaves over the past century. *Nature communications* **9**, 1–12 (2018).
10. Piatt, J. F. *et al.* Extreme mortality and reproductive failure of common murres resulting from the northeast Pacific marine heatwave of 2014-2016. *PloS one* **15**, e0226087 (2020).
11. Jacox, M. G., Alexander, M. A., Bograd, S. J. & Scott, J. D. Thermal displacement by marine heatwaves. *Nature* **584**, 82–86 (2020).
12. Morley, J. W. *et al.* Projecting shifts in thermal habitat for 686 species on the North American continental shelf. *PloS one* **13**, e0196127 (2018).
13. Perry, A. L., Low, P. J., Ellis, J. R. & Reynolds, J. D. Climate change and distribution shifts in marine fishes. *science* **308**, 1912–1915 (2005).
14. Checkley Jr, D. M. & Barth, J. A. Patterns and processes in the California Current System. *Progress in Oceanography* **83**, 49–64 (2009).

15. Bond, N. A., Cronin, M. F., Freeland, H. & Mantua, N. Causes and impacts of the 2014 warm anomaly in the NE Pacific. *Geophysical Research Letters* **42**, 3414–3420 (2015).
16. Leising, A. W. *et al.* State of the California Current 2014-15: Impacts of the Warm-Water" Blob". *California Cooperative Oceanic Fisheries Investigations Reports* **56**, 31–68 (2015).
17. McClatchie, S. State of the California Current 2015–16: comparisons with the 1997–98 El Niño. *California cooperative oceanic fisheries investigations. Data report* **57**, (2016).
18. Amaya, D. J., Miller, A. J., Xie, S.-P. & Kosaka, Y. Physical drivers of the summer 2019 North Pacific marine heatwave. *Nature communications* **11**, 1–9 (2020).
19. Weber, E. D. *et al.* State of the California current 2019–2020: Back to the future with marine heatwaves? *Frontiers in Marine Science* 1081 (2021).
20. Di Lorenzo, E. & Mantua, N. Multi-year persistence of the 2014/15 North Pacific marine heatwave. *Nature Climate Change* **6**, 1042–1047 (2016).
21. Auth, T. D., Daly, E. A., Brodeur, R. D. & Fisher, J. L. Phenological and distributional shifts in ichthyoplankton associated with recent warming in the northeast Pacific Ocean. *Global Change Biology* **24**, 259–272 (2018).
22. Brodeur, R. D., Auth, T. D. & Phillips, A. J. Major shifts in pelagic micronekton and macrozooplankton community structure in an upwelling ecosystem related to an unprecedented marine heatwave. *Frontiers in Marine Science* **6**, 212 (2019).
23. Daly, E. A., Brodeur, R. D. & Auth, T. D. Anomalous ocean conditions in 2015: impacts on spring Chinook salmon and their prey field. *Marine Ecology Progress Series* **566**, 169–182 (2017).
24. Morgan, C. A., Beckman, B. R., Weitkamp, L. A. & Fresh, K. L. Recent ecosystem disturbance in the Northern California current. *Fisheries* **44**, 465–474 (2019).
25. Peterson, W. T. *et al.* The pelagic ecosystem in the Northern California Current off Oregon during the 2014–2016 warm anomalies within the context of the past 20 years. *Journal of Geophysical Research: Oceans* **122**, 7267–7290 (2017).
26. Sakuma, K. M. *et al.* Anomalous epipelagic micronekton assemblage patterns in the neritic waters of the California Current in spring 2015 during a period of extreme ocean conditions. *CalCOFI Rep* **57**, 163–183 (2016).

27. Tanaka, K. R. *et al.* North Pacific warming shifts the juvenile range of a marine apex predator. *Scientific Reports* **11**, 3373 (2021).

28. Free, C. M. *et al.* Impact of the 2014–2016 marine heatwave on US and Canada West Coast fisheries: Surprises and lessons from key case studies. *Fish and Fisheries* (2023).

29. Frölicher, T. L. & Laufkötter, C. Emerging risks from marine heat waves. *Nature communications* **9**, 1–4 (2018).

30. Pozo Buil, M. *et al.* A dynamically downscaled ensemble of future projections for the California current system. *Frontiers in Marine Science* **8**, 612874 (2021).

31. Cheung, W. W. & Frölicher, T. L. Marine heatwaves exacerbate climate change impacts for fisheries in the northeast Pacific. *Scientific reports* **10**, 1–10 (2020).

32. Gomes, D. G. E. *et al.* An end-to-end ecosystem model of the Northern California Current. *bioRxiv* (2022) doi:https://doi.org/10.1101/2022.12.28.522165.

33. Ruzicka, J. J. *et al.* Interannual variability in the Northern California Current food web structure: changes in energy flow pathways and the role of forage fish, euphausiids, and jellyfish. *Progress in Oceanography* **102**, 19–41 (2012).

34. Ruzicka, J. J., Daly, E. A. & Brodeur, R. D. Evidence that summer jellyfish blooms impact Pacific Northwest salmon production. *Ecosphere* **7**, e01324 (2016).

35. Bizzarro, J. J. *et al.* A multi-predator trophic database for the California Current Large Marine Ecosystem. *Scientific Data* **10**, 496 (2023).

36. Steele, J. H. & Ruzicka, J. J. Constructing end-to-end models using ECOPATH data. *Journal of Marine Systems* **87**, 227–238 (2011).

37. Miller, R. R. *et al.* Distribution of pelagic thaliaceans, *Thetys vagina* and *Pyrosoma atlanticum*, during a period of mass occurrence within the California Current. *CalCOFI Rep* **60**, 94–108 (2019).

38. O'Loughlin, J. H. *et al.* Implications of *Pyrosoma atlanticum* range expansion on phytoplankton standing stocks in the Northern California Current. *Progress in Oceanography* **188**, 102424 (2020).

39. Sutherland, K. R., Sorensen, H. L., Blondheim, O. N., Brodeur, R. D. & Galloway, A. W. Range expansion of tropical pyrosomes in the northeast Pacific Ocean. *Ecology* **99**, 2397–2399 (2018).

40. Brodeur, R. D. *et al.* Demersal fish predators of gelatinous zooplankton in the Northeast Pacific Ocean. *Marine Ecology Progress Series* **658**, 89–104 (2021).

41. Doyle, T. K., Houghton, J. D., McDevitt, R., Davenport, J. & Hays, G. C. The energy density of jellyfish: estimates from bomb-calorimetry and proximate-composition. *Journal of Experimental Marine Biology and Ecology* **343**, 239–252 (2007).
42. Hays, G. C., Doyle, T. K. & Houghton, J. D. A paradigm shift in the trophic importance of jellyfish? *Trends in ecology & evolution* **33**, 874–884 (2018).
43. Heneghan, R. F., Everett, J. D., Blanchard, J. L., Sykes, P. & Richardson, A. J. Climate-driven zooplankton shifts cause large-scale declines in food quality for fish. *Nature Climate Change* 1–8 (2023).
44. Borrelli, J. J. & Ginzburg, L. R. Why there are so few trophic levels: selection against instability explains the pattern. *Food Webs* **1**, 10–17 (2014).
45. Funes, M., Saravia, L. A., Cordone, G., Iribarne, O. O. & Galván, D. E. Network analysis suggests changes in food web stability produced by bottom trawl fishery in Patagonia. *Scientific Reports* **12**, 1–10 (2022).
46. Olivier, P. *et al.* Exploring the temporal variability of a food web using long-term biomonitoring data. *Ecography* **42**, 2107–2121 (2019).
47. Elton, C. S. *The ecology of invasions by animals and plants*. (Chapman and Hall, 1958).
48. Landi, P., Minoarivelo, H. O., Brännström, Å., Hui, C. & Dieckmann, U. Complexity and stability of ecological networks: a review of the theory. *Population Ecology* **60**, 319–345 (2018).
49. May, R. M. Will a large complex system be stable? *Nature* **238**, 413–414 (1972).
50. Pimm, S. L. Food web design and the effect of species deletion. *Oikos* 139–149 (1980).
51. Pimm, S. L. The complexity and stability of ecosystems. *Nature* **307**, 321–326 (1984).
52. Dunne, J. A. The network structure of food webs. *Ecological networks: linking structure to dynamics in food webs* 27–86 (2006).
53. Dunne, J. A. Food Webs. *Encyclopedia of complexity and systems science* **1**, 3661–3682 (2009).
54. Rogers, L. A., Wilson, M. T., Duffy-Anderson, J. T., Kimmel, D. G. & Lamb, J. F. Pollock and "the Blob": Impacts of a marine heatwave on walleye pollock early life stages. *Fisheries Oceanography* **30**, 142–158 (2021).
55. Stierhoff, K. L., Zwolinski, J. P. & Demer, D. A. Distribution, Biomass, and Demography of Coastal Pelagic Fishes in the California Current Ecosystem During Summer 2019 Based on Acoustic-Trawl Sampling. *U.S. Department of Commerce, NOAA Technical Memorandum NMFS-SWFSC-626.* (2020) doi:10.25923/nghv-7c40.

56. Lindegren, M., Checkley Jr, D. M., Rouyer, T., MacCall, A. D. & Stenseth, N. C. Climate, fishing, and fluctuations of sardine and anchovy in the California Current. *Proceedings of the National Academy of Sciences* **110**, 13672–13677 (2013).

57. Lluch-Belda, D. *et al.* World-wide fluctuations of sardine and anchovy stocks: the regime problem. *South African Journal of Marine Science* **8**, 195–205 (1989).

58. Thompson, A. R. *et al.* State of the California Current Ecosystem in 2021: Winter is coming? (2022).

59. Cavole, L. M. *et al.* Biological impacts of the 2013–2015 warm-water anomaly in the Northeast Pacific: winners, losers, and the future. *Oceanography* **29**, 273–285 (2016).

60. Christensen, V. & Walters, C. J. Ecopath with Ecosim: methods, capabilities and limitations. *Ecological modelling* **172**, 109–139 (2004).

61. Ruzicka, J. J., Steele, J. H., Brink, K. H., Gifford, D. J. & Bahr, F. Understanding large-scale energy flows through end-to-end shelf ecosystems-the importance of physical context. *Journal of Marine Systems* **187**, 235–249 (2018).

62. Phillips, E. M. *et al.* Spatiotemporal variability of euphausiids in the California Current Ecosystem: insights from a recently developed time series. *ICES Journal of Marine Science* **79**, 1312–1326 (2022).

63. Epskamp, S., Cramer, A. O., Waldorp, L. J., Schmittmann, V. D. & Borsboom, D. qgraph: Network visualizations of relationships in psychometric data. *Journal of statistical software* **48**, 1–18 (2012).

64. Wickham, H. ggplot2. *Wiley Interdisciplinary Reviews: Computational Statistics* **3**, 180–185 (2011).

65. R Core Team. *R: A language and environment for statistical computing. Vienna, Austria: R Foundation for Statistical Computing*. (2017).

66. Gomes, D. G. *et al.* Why don't we share data and code? Perceived barriers and benefits to public archiving practices. *Proceedings of the Royal Society B* **289**, 20221113 (2022).

67. Gomes, D. G. E. & Ruzicka, J. J. Data and code for: Marine heatwaves disrupt ecosystem structure and function via altered food webs and energy flux. (2023) doi:10.5281/ZENODO.8121889.

68. Gomes, D. & Ruzicka, J. ECOTRAN CODE: NCC2-2D. (2023) doi:10.5281/ZENODO.8140850.

69. Gomes, D. G. E. & Ruzicka, J. J. Data and Code for 'An updated end-to-end ecosystem model of the Northern California Current'. (2022) doi:10.5281/zenodo.8015467.

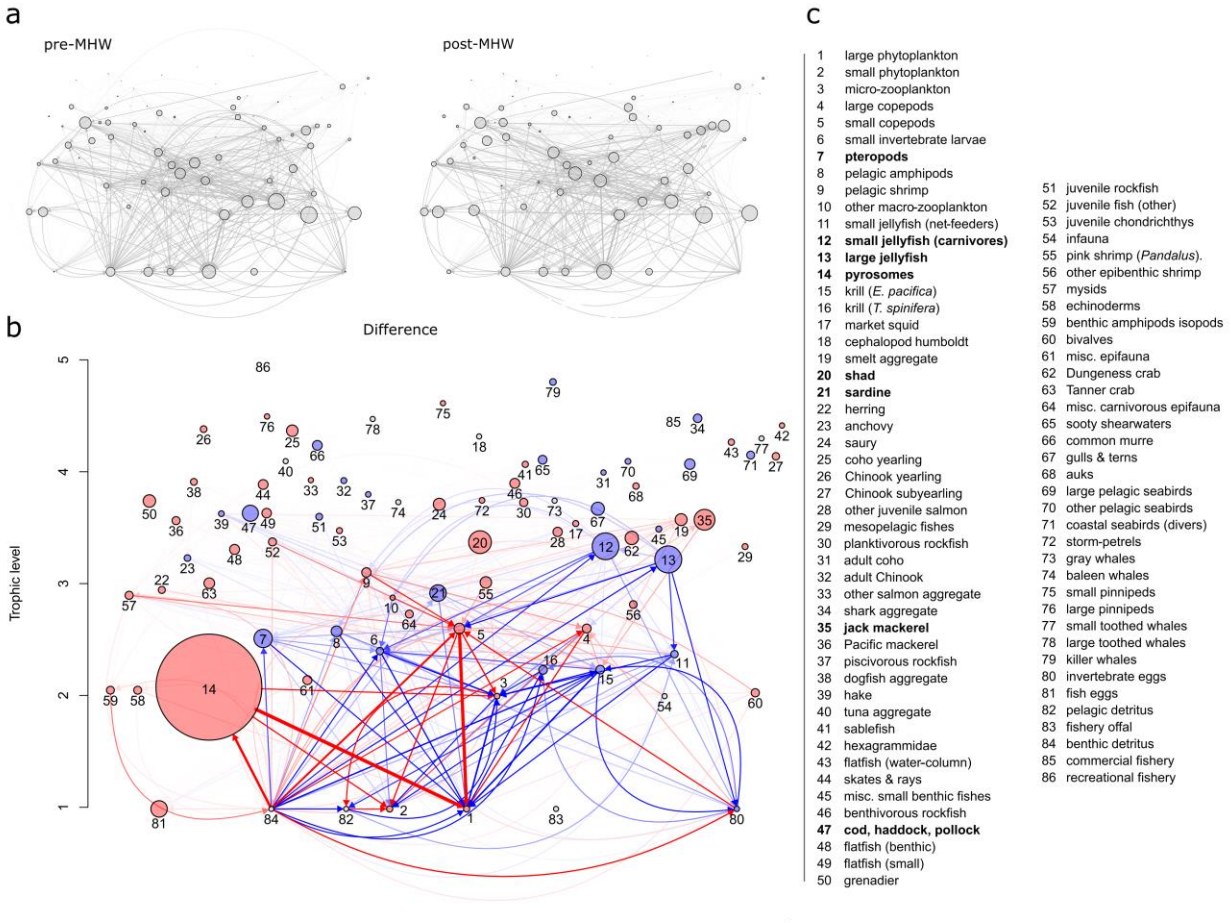

Figure 1. Consumption matrix difference between pre-MHW and post-MHW food webs. a, Pre-MHW and post-MHW network diagrams show the food web consumption matrix. Trophic linkages (network edges) show rates of biomass exchange between trophic levels while the size of circles (network nodes) represent the absolute biomass densities in the system (on the log scale; see **Table S1**). **b**, A "difference" network was calculated as the difference between the pre-MHW model and the post-MHW model for both the edge weights and node biomasses. Node and edge sizes and colors depend on the magnitude and direction of change, respectively. Red colors indicate an increase from the pre-MHW food web to the post-MHW food web, while blue colors indicate a decrease. The size of the circle corresponds to the magnitude of the change in biomass of a given functional group (indicated by the corresponding number, see **Table S1**). Similarly, the thickness and color intensity of the lines (network edges) indicate the magnitude of change in energy flux between food webs. Node locations are identical in all three networks. The node numbers were omitted from the top two plots for easier visualization. **c**, A list of functional groups in ecosystem models, with bolded names selected to highlight those with larger changes between model time periods.

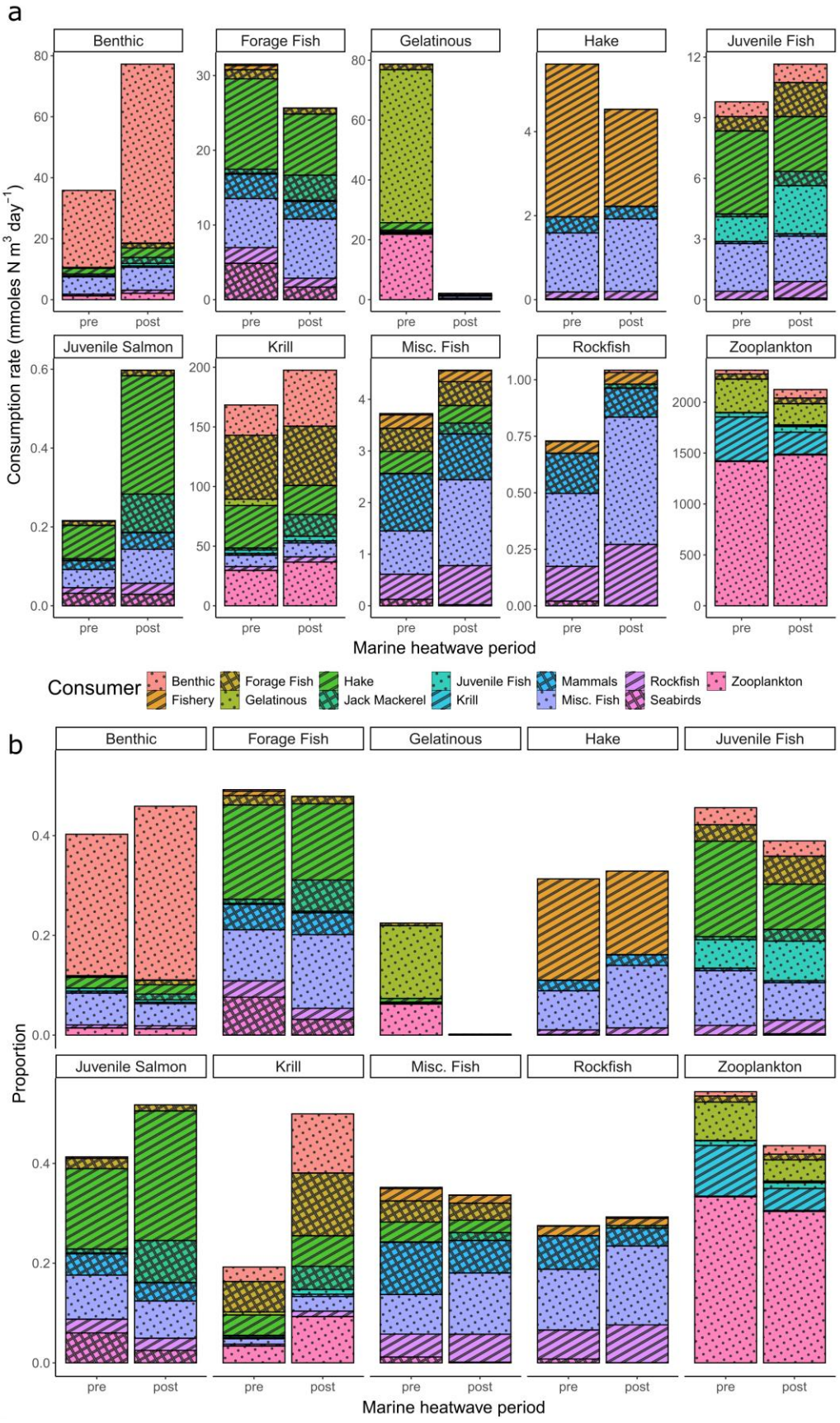

Figure 2. Bottom-up energy flow through ecosystem functional groups. The x-axis in both panels indicates the pre- vs post-MHW time period. **a**, The y-axis is the absolute consumption rate of specific functional groups (indicated in boxes across top of panel facets) by consumer groups (see legend for color-pattern combinations) in units of mmol N per cubic meter per day. **b**, The y-axis shows the proportion of consumption that is allocated from specific functional groups to living consumer group types. All non-living nutrients and detritus pool groups were removed from these plots of energy transfer, because the ending fate of much of the system energy ends up in these pools, obscuring patterns in non-detritus groups. Thus, note that the y-axis in panel b does not extend to 1. A representative subset of taxa is presented.

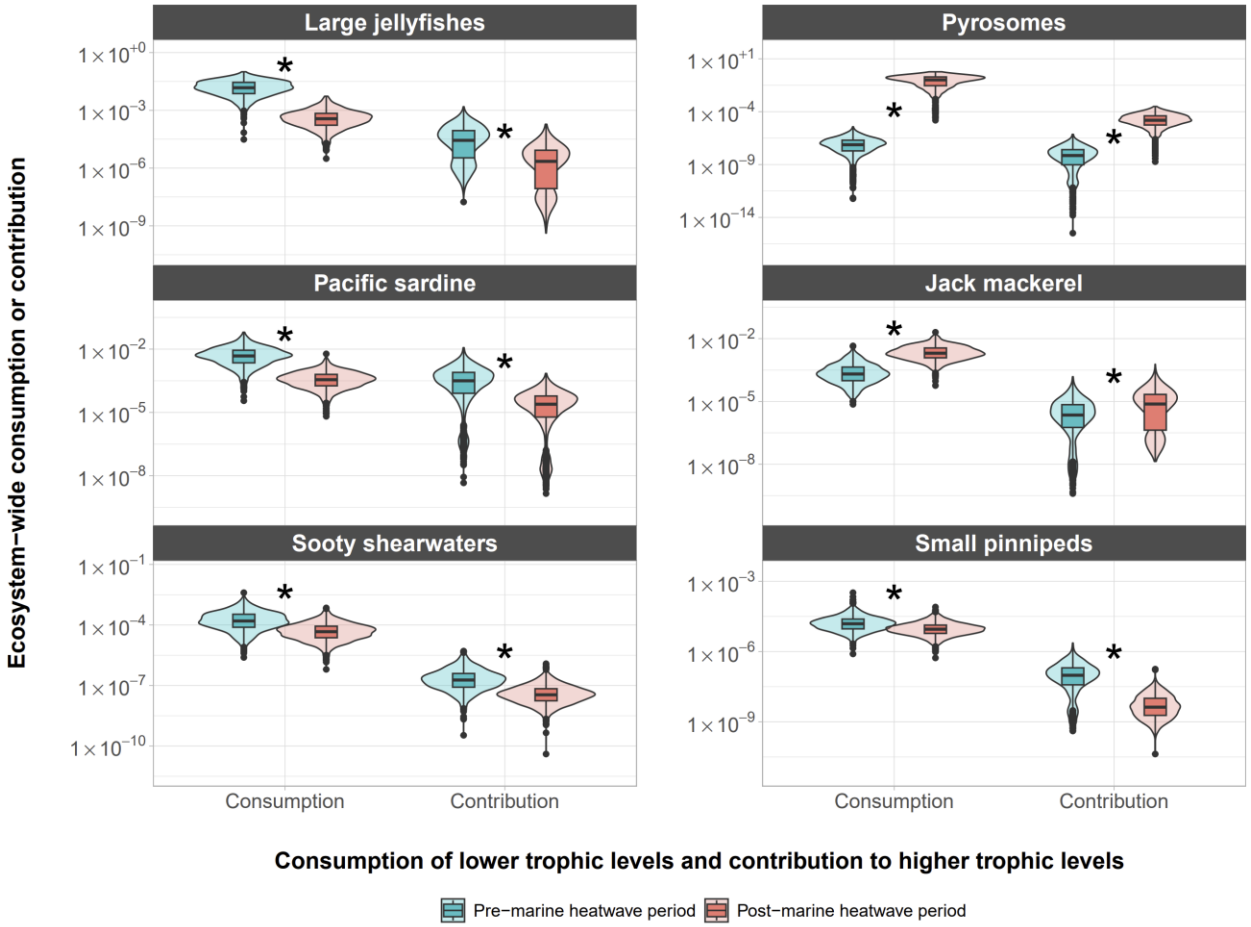

Figure 3. Ecosystem-wide consumption and contribution values for representative taxa. Violin plots show density of points from 1000 Monte Carlo runs of ecosystem models. Blue indicates values for the consumption of prey (functional groups as consumers) and red indicates contribution to predators (functional groups as producers). Plotted over the violin plots, boxplots show median values as thick horizontal lines and first and third quartiles (the 25th and 75th percentiles) as the lower and upper edges of the box, respectively. The lower and upper whiskers extend from the edges of the box to the values that are smallest and largest (respectively), yet no further than 1.5 × interquartile range (i.e., the distance between the first and third quartiles) from the box. Outlying data beyond the end of the whiskers are plotted as individual points. Asterisks indicate that the difference in consumption of prey and contribution to predators between the pre- and post-MHW models is significantly different. See supplement for visualization of other functional groups.

Statistic	Pre-MHW	Post-MHW	p value	t value	df
Number of nodes	86	86	–	–	–
Mean Trophic Level (TL)	3.268	3.288	0.90	-0.128	169.8
TL weighted by biomass	2.339	2.413	0.63	-0.481	169.8
Connectance	0.229	0.251	2.15×10^{-10}	6.698	197.8
Link density (links per node)	19.709	21.605	2.15×10^{-10}	6.698	197.8

Table 1. Network stability metrics. Comparison between pre- and post-MHW ecosystem model network values. Two-tailed T-test outputs are reported as p values, t values, and degrees of freedom (df). Connectance = the number of (non-zero) realized links relative to the total number of possible links (86×86=7396). None of the calculations include nutrients as functional groups.

Supplementary Information

Marine heatwaves disrupt ecosystem structure and function via altered food webs and energy flux

Dylan G.E. Gomes, James J. Ruzicka, Lisa G. Crozier, David D. Huff, Richard D. Brodeur, Joshua D. Stewart

Corresponding author: dylan.ge.gomes@gmail.com

The PDF file includes:

Figures S1 to S5
Table S1

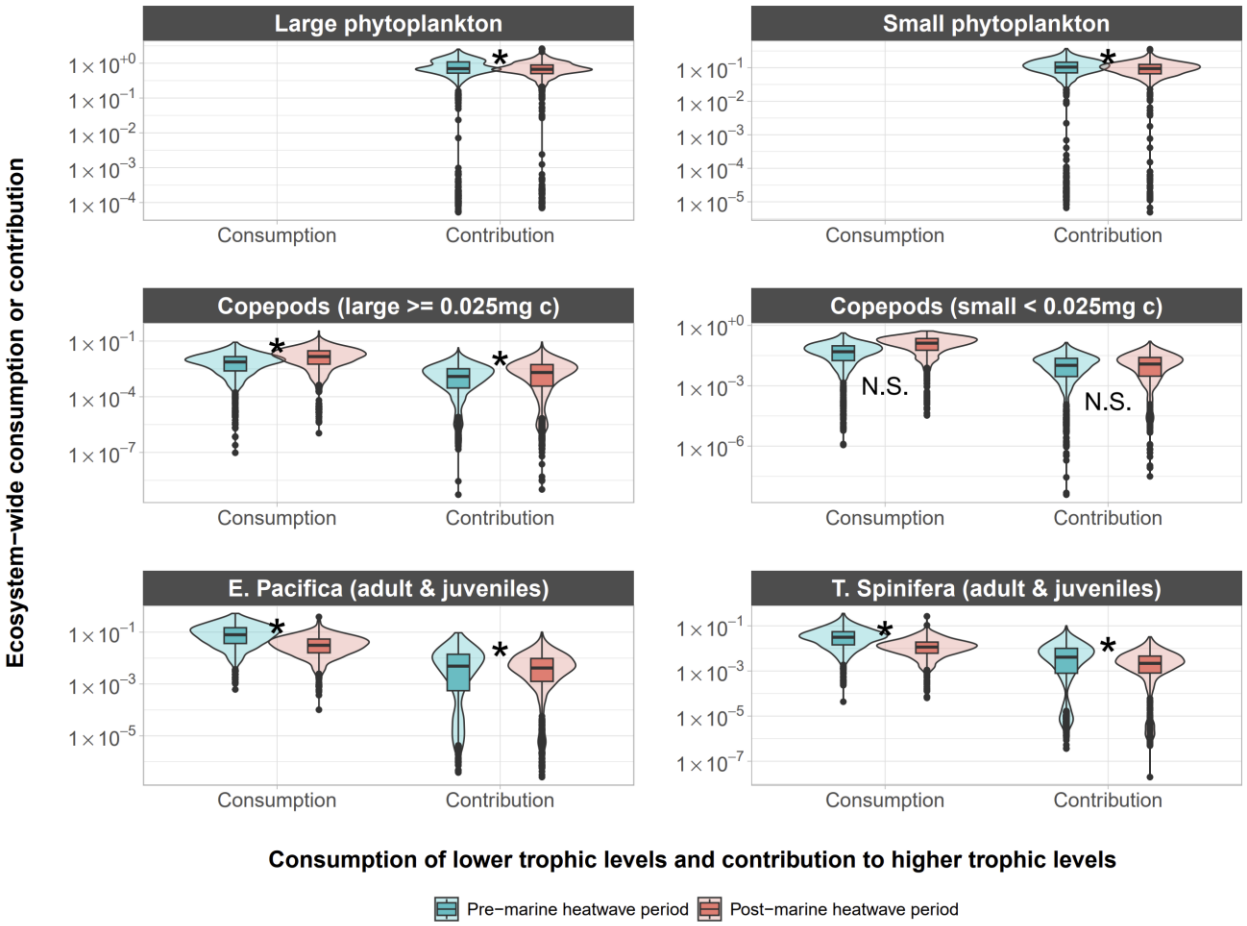

Figure S1. Ecosystem-wide consumption of prey and contribution to predators of lower trophic levels.

Violin plots show density of points. Plotted over the violin plots, boxplots show median values as thick horizontal lines and first and third quartiles (the 25th and 75th percentiles) as the lower and upper edges of the box, respectively. The lower and upper whiskers extend from the edges of the box to the values that are smallest and largest (respectively), yet no further than 1.5 × interquartile range (i.e., the distance between the first and third quartiles) from the box. Outlying data beyond the end of the whiskers are plotted as individual points. Asterisks indicate that the difference in consumption of prey (footprint) and contribution to predators (reach) between the pre- and post-MHW models is significantly different.

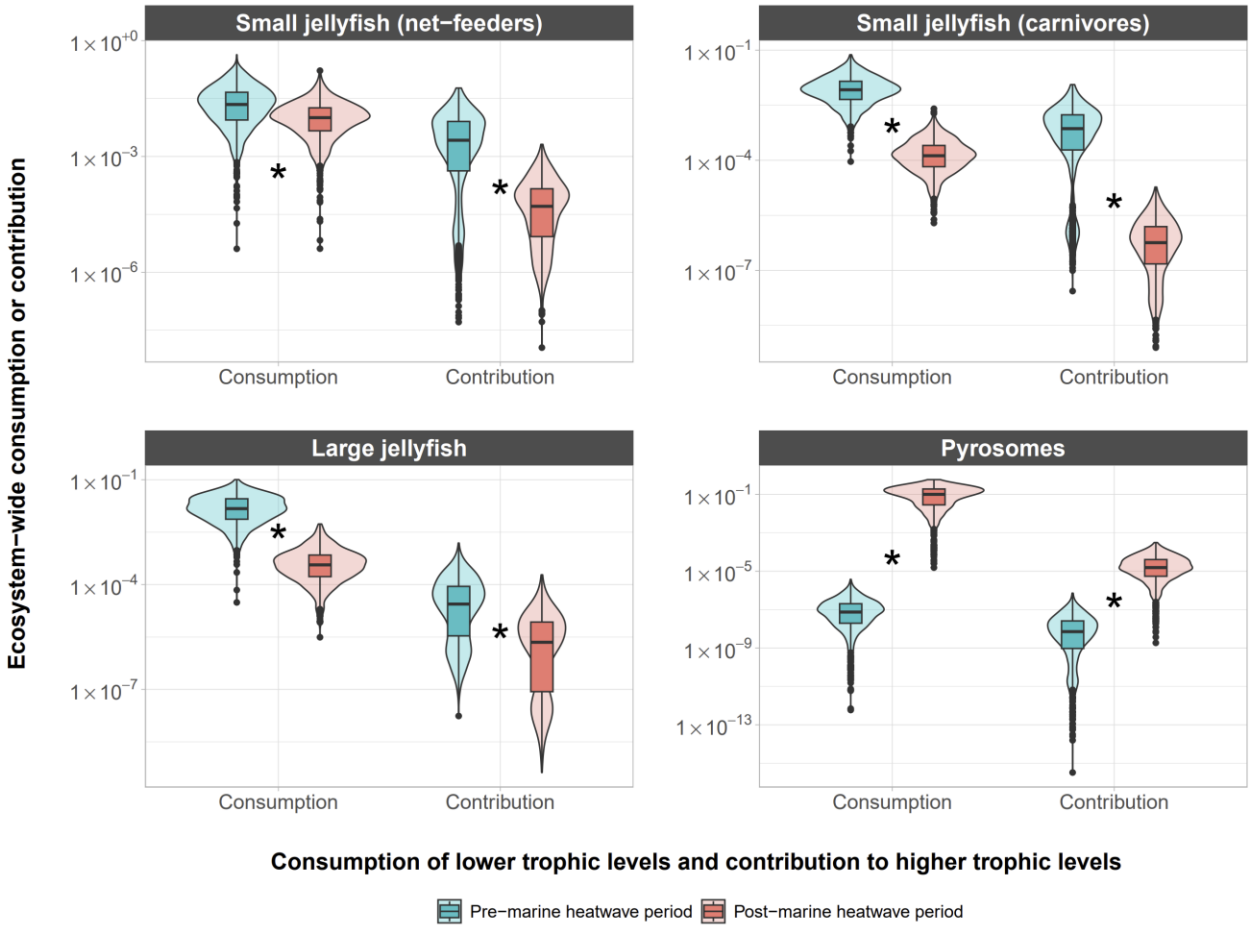

Figure S2. Ecosystem-wide consumption of prey and contribution to predators of gelatinous animals.

Violin plots show density of points. Plotted over the violin plots, boxplots show median values as thick horizontal lines and first and third quartiles (the 25th and 75th percentiles) as the lower and upper edges of the box, respectively. The lower and upper whiskers extend from the edges of the box to the values that are smallest and largest (respectively), yet no further than 1.5 × interquartile range (i.e., the distance between the first and third quartiles) from the box. Outlying data beyond the end of the whiskers are plotted as individual points. Asterisks indicate that the difference in consumption of prey (footprint) and contribution to predators (reach) between the pre- and post-MHW models is significantly different.

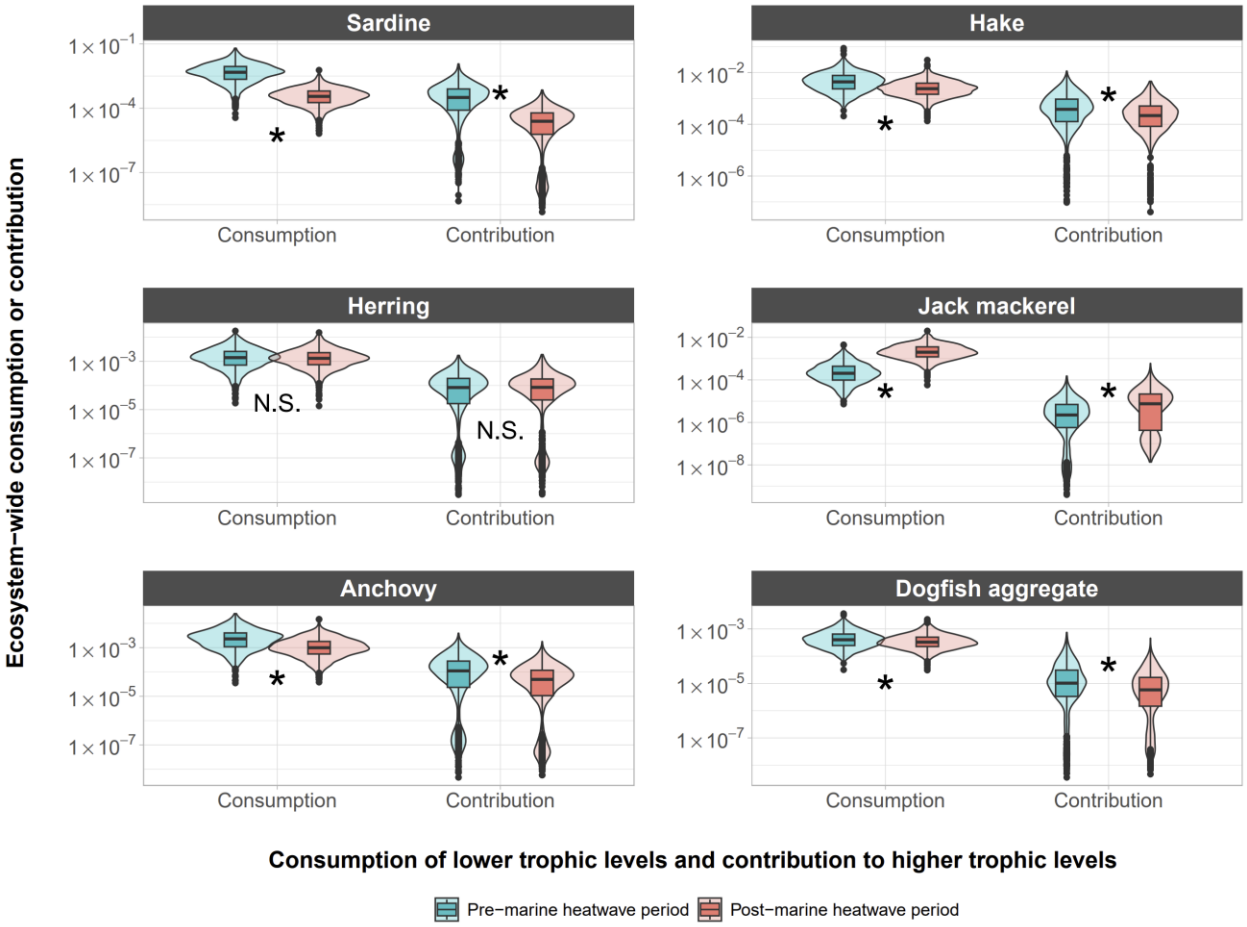

Figure S3. Ecosystem-wide consumption of prey and contribution to predators of various fishes.

Violin plots show density of points. Plotted over the violin plots, boxplots show median values as thick horizontal lines and first and third quartiles (the 25th and 75th percentiles) as the lower and upper edges of the box, respectively. The lower and upper whiskers extend from the edges of the box to the values that are smallest and largest (respectively), yet no further than 1.5 × interquartile range (i.e., the distance between the first and third quartiles) from the box. Outlying data beyond the end of the whiskers are plotted as individual points. Asterisks indicate that the difference in consumption of prey (footprint) and contribution to predators (reach) between the pre- and post-MHW models is significantly different.

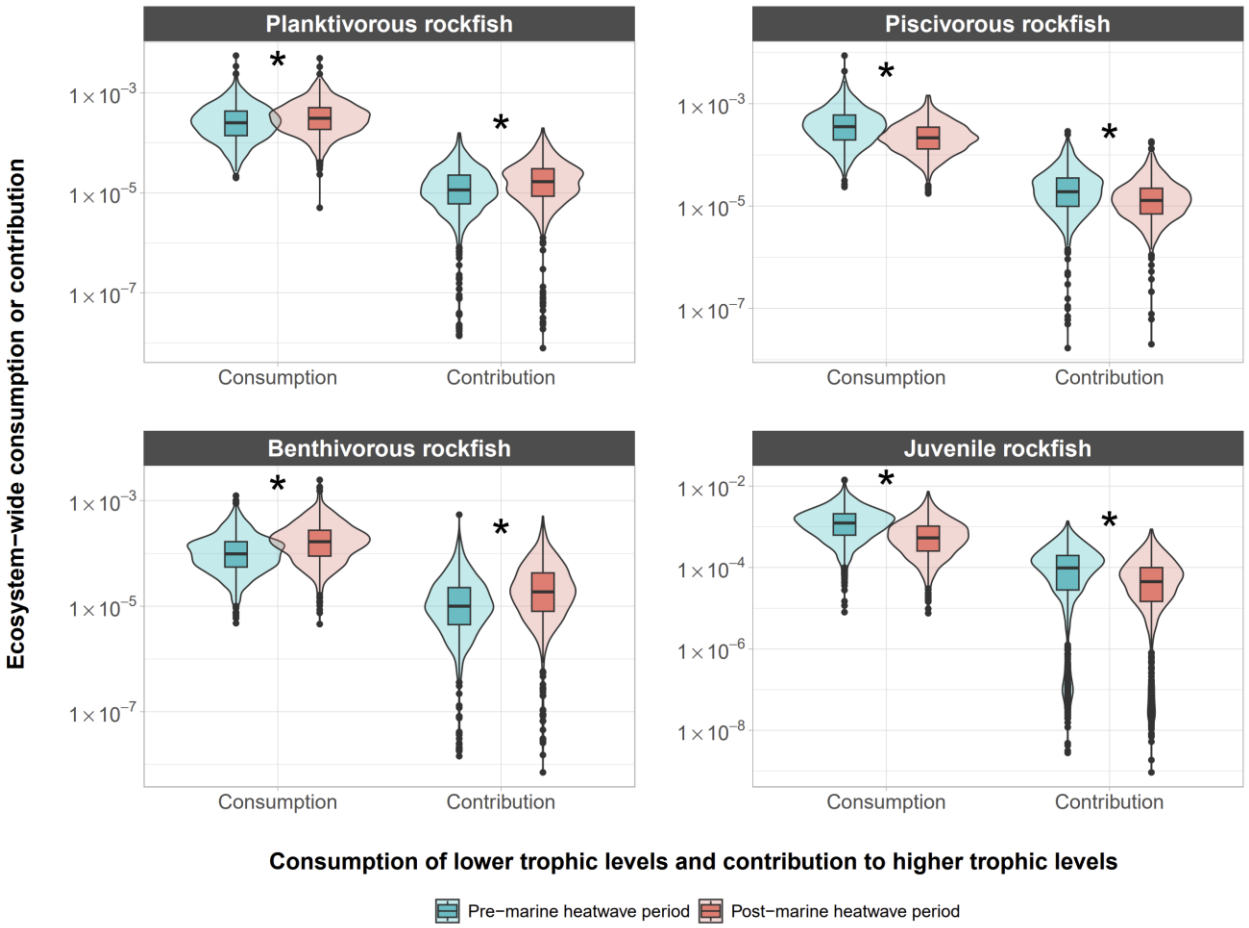

Figure S4. Ecosystem-wide consumption of prey and contribution to predators of rockfishes.

Violin plots show density of points. Plotted over the violin plots, boxplots show median values as thick horizontal lines and first and third quartiles (the 25th and 75th percentiles) as the lower and upper edges of the box, respectively. The lower and upper whiskers extend from the edges of the box to the values that are smallest and largest (respectively), yet no further than 1.5 × interquartile range (i.e., the distance between the first and third quartiles) from the box. Outlying data beyond the end of the whiskers are plotted as individual points. Asterisks indicate that the difference in consumption of prey (footprint) and contribution to predators (reach) between the pre- and post-MHW models is significantly different.

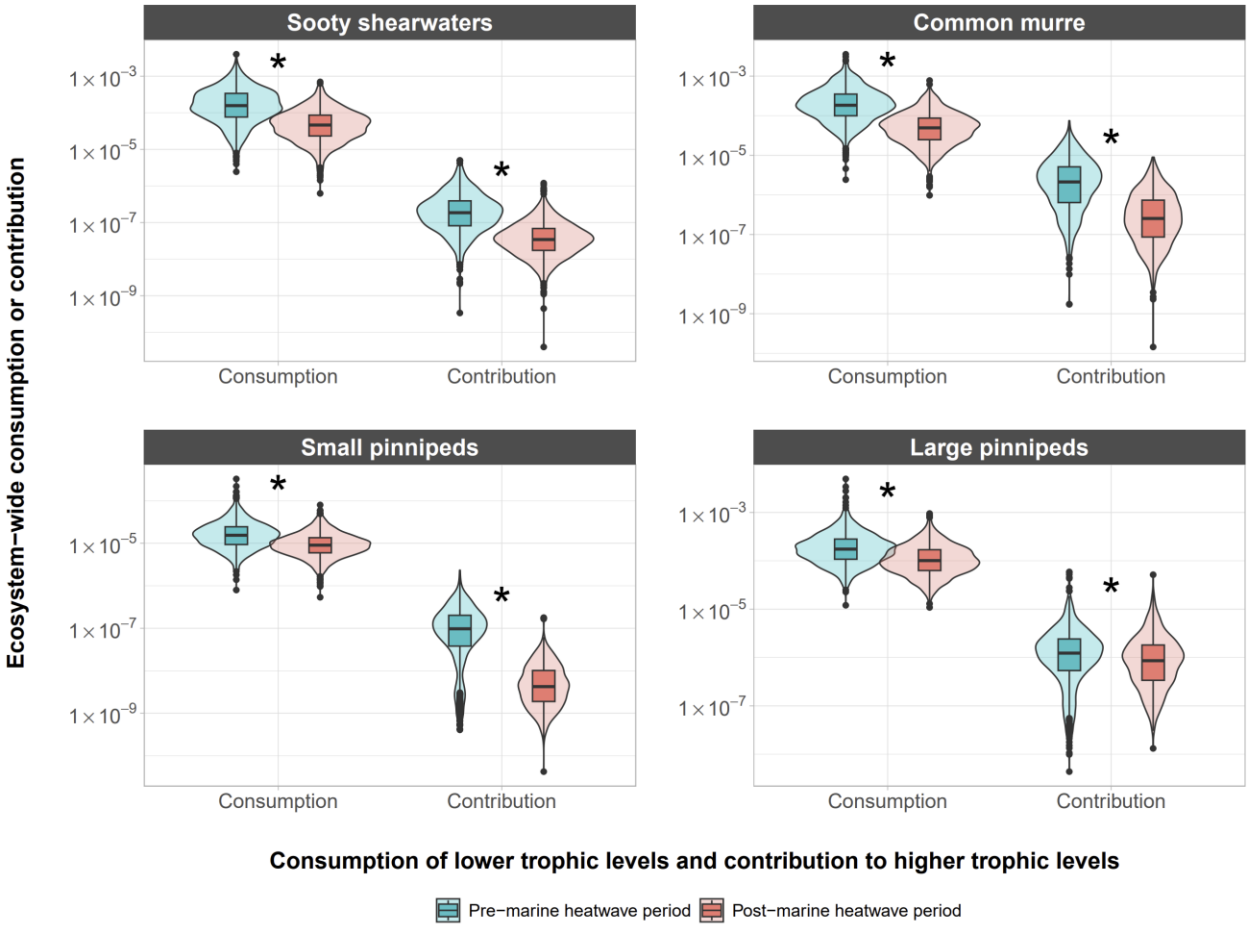

Figure S5. Ecosystem-wide consumption of prey and contribution to predators of seabird and mammal predators.

Violin plots show density of points. Plotted over the violin plots, boxplots show median values as thick horizontal lines and first and third quartiles (the 25th and 75th percentiles) as the lower and upper edges of the box, respectively. The lower and upper whiskers extend from the edges of the box to the values that are smallest and largest (respectively), yet no further than 1.5 × interquartile range (i.e., the distance between the first and third quartiles) from the box. Outlying data beyond the end of the whiskers are plotted as individual points. Asterisks indicate that the difference in consumption of prey (footprint) and contribution to predators (reach) between the pre- and post-MHW models is significantly different.

Table S1. Ecosystem model parameter comparison.

Ecopath parameterization of pre-MHW and post-MHW models. Years represent focus dates for representing biomass in the system (see Methods). TL = estimated trophic level, Biomass = calculated (or estimated) average biomass density in ecosystem (mt/km2), EE = ecotrophic efficiency, PB = biomass-specific production rate, CB = biomass-specific consumption rate. EE values are estimated by the Ecopath master equation (see Gomes et al. 2022; *30*), except those in which biomass was estimated (EE in bold are fixed). See data and code for .csv version.

		Pre-MHW (1999 - 2012)			Post-MHW (2014 - 2022)			Shared parameters	
	Functional Group	TL	Biomass	EE	TL	Biomass	EE	PB	CB
1	large phytoplankton	1.00	34.938	0.965	1.00	45.753	0.98	215.00	
2	small phytoplankton	1.00	4.757	0.973	1.00	6.230	0.945	215.00	
3	micro-zooplankton	2.00	13.940	**0.9**	2.00	16.219	**0.9**	150.00	428.57
4	large copepods	2.60	2.834	0.86	2.25	6.552	0.744	15.00	60.00
5	small copepods	2.60	8.325	0.948	2.35	26.443	0.419	37.00	148.00
6	small invertebrate larvae	2.40	8.178	0.842	2.35	4.813	0.573	37.00	148.00
7	pteropods	2.51	2.929	0.649	2.53	0.272	0.759	15.00	50.00
8	pelagic amphipods	2.58	2.174	**0.85**	2.65	0.662	0.732	14.00	56.00
9	pelagic shrimp	3.10	7.494	**0.85**	3.27	18.939	0.885	3.00	12.00
10	other macro-zooplankton	2.87	6.128	0.763	2.88	6.309	0.725	10.00	40.00
11	small jellyfish (mesh-feeders)	2.37	2.818	0.509	2.40	1.671	0.021	45.00	150.00
12	small jellyfish (carnivores)	3.33	1.910	0.509	3.48	0.054	0.023	20.00	66.67
13	large jellyfish	3.21	3.748	0.021	3.08	0.101	0.079	15.00	60.00
14	pyrosomes	2.08	0.00001	0.694	2.08	15.976	0.001	45.00	150.00
15	*E. pacifica* (adult & juveniles)	2.24	70.723	0.329	2.30	32.294	0.931	6.00	24.00
16	*T. spinifera* (adult & juveniles)	2.23	22.414	0.399	2.30	10.234	0.799	7.00	28.00
17	small cephalopods	3.53	2.116	**0.85**	3.63	2.640	**0.85**	3.00	12.00
18	Humboldt squid	4.30	0.005	0.785	4.36	0.005	0.969	2.75	11.00
19	smelt aggregate	3.57	1.846	0.91	3.65	7.383	0.819	1.80	7.20
20	shad	3.37	0.102	0.854	3.34	2.081	**0.9**	1.13	4.53
21	sardine	2.91	15.203	0.877	3.11	1.841	0.966	1.13	4.53
22	herring	2.94	2.613	0.911	3.17	4.099	0.943	1.80	7.20
23	anchovy	3.22	4.339	0.91	3.19	3.038	0.888	1.80	7.20
24	saury	3.70	0.032	0.843	3.75	0.130	0.792	1.13	4.53
25	coho yearling	4.35	0.060	0.909	4.28	0.222	0.933	1.80	7.20
26	Chinook yearling	4.37	0.080	0.531	4.22	0.119	0.937	1.80	7.20
27	Chinook subyearling	4.13	0.035	0.909	4.04	0.059	0.956	1.80	7.20
28	other juvenile salmon	3.46	0.011	0.909	3.41	0.028	0.855	1.80	7.20
29	mesopelagic fish aggregate	3.33	1.000	0.797	3.36	1.245	**0.85**	1.75	7.00
30	planktivorous rockfish	3.72	3.152	0.908	3.76	6.420	0.952	0.13	1.25
31	coho	3.98	0.240	0.893	4.17	0.230	0.739	1.80	10.59
32	Chinook	3.91	0.138	0.918	4.07	0.112	0.892	0.75	4.41
33	other salmon aggregate	3.92	0.018	0.93	3.98	0.019	0.756	1.90	11.18
34	shark aggregate	4.46	0.037	0.611	4.73	0.017	0.788	0.20	3.33
35	jack mackerel	3.56	1.389	0.626	3.64	21.395	0.103	0.23	2.30
36	Pacific mackerel	3.56	0.436	0.637	3.49	0.857	0.848	0.76	7.60

		Pre-MHW (1999 - 2012)			Post-MHW (2014 - 2022)			Shared parameters	
	Functional Group	TL	Biomass	EE	TL	Biomass	EE	PB	CB
37	piscivorous rockfish	3.79	3.398	0.948	3.88	3.072	0.98	0.17	1.72
38	dogfish aggregate	3.90	2.330	0.64	4.20	3.475	0.272	0.20	2.50
39	hake	3.62	21.808	0.94	3.65	18.500	0.987	0.35	3.54
40	tuna aggregate	4.08	0.200	0.84	4.29	0.200	0.893	0.30	3.00
41	sablefish	4.06	1.358	0.838	4.16	1.787	0.952	0.23	2.30
42	hexagrammidae (lingcod greenling)	4.40	0.688	0.891	4.43	0.722	0.905	0.30	3.00
43	flatfish (water-column feeders)	4.25	2.833	0.919	4.29	3.797	0.817	0.28	1.38
44	skates & rays	3.88	1.017	0.729	3.71	2.769	0.266	0.23	2.30
45	misc. small benthic fishes	3.48	11.109	**0.85**	3.33	8.900	**0.9**	0.40	4.00
46	benthivorous rockfish	3.89	2.845	0.845	3.67	7.987	0.811	0.07	0.70
47	gadidae (cod haddock pollock)	3.62	0.926	**0.85**	3.48	0.120	0.838	0.35	3.50
48	flatfish (benthic feeders)	3.30	4.188	0.908	3.16	11.878	0.684	0.30	3.00
49	flatfish (small)	3.62	3.080	0.937	3.45	7.968	0.919	0.38	1.90
50	grenadier	3.73	0.277	0.833	3.62	1.206	0.066	0.20	1.00
51	juvenile rockfish	3.59	1.809	**0.85**	3.51	1.202	0.933	2.70	10.80
52	juvenile fish (other)	3.37	3.044	**0.85**	3.26	5.991	0.692	2.70	10.80
53	juvenile fish (chondrichthys)	3.47	0.427	**0.85**	3.44	0.535	**0.85**	2.70	10.80
54	infauna	2.00	80.000	0.607	2.00	80.000	0.973	4.50	18.00
55	Pandalus spp.	3.01	3.873	**0.85**	2.91	14.257	0.903	3.00	12.00
56	other epibenthic shrimp	2.81	7.237	**0.85**	2.81	12.948	**0.85**	4.20	16.80
57	mysids	2.89	1.323	**0.85**	2.83	2.637	**0.85**	22.00	110.00
58	echinoderms	2.05	11.180	**0.85**	2.07	21.359	**0.85**	1.21	6.05
59	other benthic crustaceans	2.05	3.804	**0.85**	2.05	7.157	**0.85**	21.50	107.50
60	bivalves	2.03	31.667	**0.85**	2.03	64.443	**0.85**	1.30	6.50
61	suspension-feeding epifauna	2.14	1.625	**0.85**	2.14	3.827	**0.85**	7.40	37.00
62	Dungeness crab	3.40	1.017	0.951	3.27	5.109	0.952	1.50	6.00
63	Tanner crab	3.00	0.270	0.944	2.99	0.869	0.939	1.00	4.00
64	other carnivorous epifauna	2.73	16.515	**0.85**	2.67	31.546	**0.85**	3.00	15.00
65	sooty shearwaters	4.10	0.039	0.105	4.31	0.017	0.014	0.10	73.00
66	common murre	4.22	0.041	0.447	4.37	0.015	0.21	0.17	72.00
67	gulls & terns	3.66	0.005	0.52	3.79	0.001	0.774	0.17	73.00
68	alcids	3.86	0.001	0.411	3.90	0.001	0.084	0.17	110.00
69	large pelagic seabirds	4.06	0.003	0.754	4.08	0.001	0.128	0.07	75.00
70	other pelagic seabirds	4.08	0.001	0.702	4.29	0.001	0.046	0.10	73.00
71	coastal seabirds (divers)	4.14	0.001	0.411	4.29	0.001	0.218	0.16	73.00
72	storm-petrels	3.74	0.0001	0.411	3.86	0.0001	0.072	0.12	144.00
73	gray whales	3.73	0.146	0.044	3.72	0.146	0.002	0.06	8.90
74	baleen whales	3.72	0.572	0.036	3.69	0.572	0.002	0.04	7.60
75	small pinnipeds	4.60	0.023	0.632	4.55	0.024	0.034	0.08	8.30
76	large pinnipeds	4.48	0.105	0.666	4.56	0.111	0.245	0.07	24.00
77	small toothed whales	4.29	0.072	0.57	4.44	0.072	0.112	0.10	25.80
78	large toothed whales	4.46	0.067	0.052	4.57	0.067	0.003	0.05	6.61
79	killer whales	4.79	0.007	0	5.11	0.005	0	0.03	11.16
80	invertebrate eggs	1.00	0.000019	0.763	1.00	0.000018	0.225	-	-
81	fish eggs	1.00	0.234	0.995	1.00	1.906	0.422	-	-

		Pre-MHW (1999 - 2012)			Post-MHW (2014 - 2022)			Shared parameters	
	Functional Group	TL	Biomass	EE	TL	Biomass	EE	PB	CB
82	pelagic detritus	1.00	10.000	0.368	1.00	10.000	0.524	-	-
83	fishery offal	1.00	5.000	0.555	1.00	5.000	0.684	-	-
84	benthic detritus	1.00	10.000	0.808	1.00	10.000	0.884	-	-
85	Commercial	4.52	-	-	4.58	-	-	-	-
86	recreational fishery	5.01	-	-	5.07	-	-	-	-